DOI: 10.1002/ejic.200901013

New Mixed-Valence $Mn^{II/III}_6$ Complexes Bearing Oximato and Azido Ligands: Synthesis, and Structural and Magnetic Characterization

Christos Lampropoulos,[a] Theocharis C. Stamatatos,[a] Manolis J. Manos,[b] Anastasios J. Tasiopoulos,[b] Khalil A. Abboud,[a] and George Christou*[a]

Keywords: Mixed-valent compounds / Polynuclear complexes / Manganese / Azides / Magnetic properties

The combined use of the anion of methyl 2-pyridyl ketone oxime ($mpko^-$) and azides (N_3^-) in non-carboxylate Mn chemistry has afforded two new Mn_6 clusters, $[Mn_6O_3(N_3)_3(mpko)_6(H_2O)_3](ClO_4)_2$ (**1**) and $[Mn_6O_3(N_3)_5(mpko)_6(H_2O)]$ (**2**), which are mixed-valence (Mn^{II}, 5 Mn^{III}). The 1:1:1:1 reaction of $Mn(ClO_4)_2{\cdot}6H_2O$, mpkoH, NaN_3 and NEt_3 in MeOH gave the cationic complex **1**, while a similar reaction using additional NaO_2CMe led instead to the neutral complex **2**. The structurally unprecedented cores of the two cages are very similar, and contain the six Mn ions in a topology comprising three vertex-sharing oxide-centered triangles bridged by two end-on azides. Variable-temperature, solid-state dc and ac magnetization studies were carried out for **1** and **2** in the 1.8–300 K range. The data reveal $S = 5/2$ ground states for both complexes, and fitting of magnetization vs. field (H) and temperature (T) data by matrix diagonalization for **1** gave $S = 5/2$, $D = -1.4(3)$ cm^{-1}, and $g = 1.99(1)$, where D is the axial zero-field splitting (ZFS) parameter. The combined results demonstrate the versatility of 2-pyridyl ketone oxime anions in the presence of suitable ancillary ligands, such as azides, for the synthesis of new Mn clusters, without requiring the co-presence of carboxylate ligands.

Introduction

The synthesis of polynuclear transition-metal clusters has become attractive to many inorganic chemists for a variety of reasons: (i) the relevance of metal clusters to bioinorganic chemistry and the synthesis of models for various active sites found in nature,[1] such as the water oxidizing complex in Photosystem II,[2] the inorganic center of ferritin,[3] the active site of nitrogenase[4] and others, and (ii) the magnetic properties of such clusters when comprised of paramagnetic metal ions. This latter field has flourished since the discovery of single-molecule magnetism, where every molecule behaves as a magnetic nanoparticle below a blocking temperature (T_B).[5] These molecules exhibit both the classical properties of a magnet (i.e. hysteresis loops in magnetization vs. field studies) and quantum properties such as quantum tunneling of the magnetization, mainly originating from their nanoscale dimensions.[6] The main requirements for single-molecule magnets (SMMs) are the presence of a large ground-state spin, S, and a significant magnetoanisotropy of the Ising (easy-axis) type, reflected in a large and negative zero-field splitting parameter, D. Manganese has been the metal of choice for the synthesis of SMMs, due to the significant molecular anisotropy originating from the Jahn–Teller distorted Mn^{III} ions.[7] To date, the most well-studied SMMs are the carboxylate-bridged clusters of formula $[Mn_{12}O_{12}(O_2CR)_{16}(L)_4]$ (R = various, L = terminal ligands),[8] but many others have also been synthesized and characterized.[9] Many synthetic routes have been reported for the synthesis of 3d-metal clusters and SMMs, most of which involve the reactions of simple metal salts with bridging/chelating organic ligands under basic conditions.[10] Also, the employment of ferromagnetic couplers, such as $\mu_{1,1}$ (end-on) bridging azide (N_3^-) groups, in the reactions has been proven very successful for the synthesis of molecular species with high-spin ground states,[11,14] one of the requirements for SMMs.

Many types of organic ligands have been used in Mn chemistry, most of which have been alcoholates or polyalcoholates,[11a,11b,11g,12] and oximes and dioximes.[13,17] Thus, the combinatory use of suitable bridging/chelating agents and ancillary ligands, such as carboxylates and/or azides has provided access to very interesting metal clusters with unprecedented topologies, some of which possess very high-spin ground states (currently up to 83/2)[14] and large metal nuclearities, currently up to Mn_{40}.[15] One particular class of chelates, namely the oximato-based ligands, although typically producing smaller complexes with metal nuclearities currently up to 14,[16] has been very attractive to synthetic inorganic chemists, due to the flexibility of the oximato (>C=N–O$^-$) arm(s). In particular, methyl 2-pyridyl ketone oxime (mpkoH) was used for the synthesis of the first triangular Mn^{III}_3 SMMs,[17] while salicylaldoxime

[a] Department of Chemistry, University of Florida, Gainesville, Florida 32611-7200, USA
Fax: +1-352-392-6737
E-mail: christou@chem.ufl.edu
[b] Department of Chemistry, University of Cyprus, 1678 Nicosia, Cyprus

Supporting information for this article is available on the WWW under http://dx.doi.org/10.1002/ejic.200901013.

($saoH_2$) and its R-substituted derivatives (R-$saoH_2$; R = Me, Et, Ph, etc) have produced many Mn SMMs with large energy barriers for magnetization reversal (Scheme 1).[13a–13c,18]

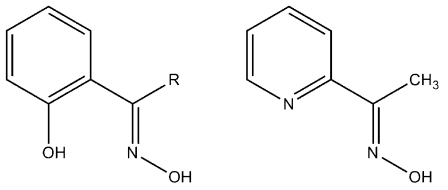

R-$saoH_2$ mpkoH

Scheme 1. The organic ligands discussed in the text.

Thus, extending our previous studies using a wide range of pyridyl alcohols, 2-pyridyl oximes and dioximes in Mn chemistry, we herein report the syntheses of two new hexanuclear Mn clusters incorporating the anions of $mpko^-$ and N_3^-.

Results and Discussion

Syntheses

Several synthetic methodologies to Mn clusters have been employed to date, many of which employ reactions of carboxylate starting materials, either simple Mn^{II} carboxylate salts (i.e. $Mn(O_2CR)_2$) or preformed Mn^{III} or $Mn^{III/IV}$ clusters, such as $[Mn_3O(O_2CR)_6L_3]^{0/+}$, $[Mn_4O_2(O_2CPh)_9(H_2O)]^-$, and/or $[Mn_{12}O_{12}(O_2CR)_{16}L_4]$ (R = various and L = terminal ligand), with a potentially bridging and/or chelating ligand.[10,13,17,18] In particular, polyols and pyridyl alcohols have been invaluable in Mn chemistry,[11,12,19] providing access to many structurally novel clusters, some of which are SMMs. Another fruitful ligand type in Mn chemistry is the broad family of oximato-based chelates, such as the pyridyl oximes.[20] In the present study, we have investigated the reactivity of *non-carboxylate* Mn^{II} salts, i.e. $Mn(ClO_4)_2{\cdot}6H_2O$, with the bridging/chelating mpkoH ligand in combination with azides; the latter group is also an excellent bridging ligand that can foster the formation of high nuclearity products,[11,21] some with extremely large *S* values.

Various reactions have been systematically explored with differing reagent ratios, reaction solvents, and other conditions. The 1:1:1 reaction between $Mn(ClO_4)_2{\cdot}6H_2O$, NaN_3 and mpkoH in MeOH in the presence of one equivalent of NEt_3 led to a dark brown solution and the subsequent isolation of well-formed brown crystals of $[Mn_6O_3(N_3)_3(mpko)_6(H_2O)_3](ClO_4)_2{\cdot}5H_2O$ (**1**·$5H_2O$) in good yield (≈ 50%). Complex **1** is a mixed-valent $Mn^{II}Mn^{III}_5$ species; the Mn^{III} ions were clearly formed by aerial oxidation of Mn^{II} under the prevailing basic conditions. The basic character of azide groups and the well-known ability of $mpko^-$ to favor formation of Mn^{III} over Mn^{II} no doubt also facilitated the oxidation of Mn^{II} to Mn^{III} to give **1**. When the same reaction was repeated using $Mn(NO_3)_2{\cdot}H_2O$ in place of $Mn(ClO_4)_2{\cdot}6H_2O$, the yield of the corresponding nitrate version of **1** (complex **3**, see Exp. Sect.) dropped significantly to ca. 10–15%. As with many reactions in higher oxidation state Mn chemistry, the solution likely contains a mixture of species in equilibrium, and what crystallizes out is determined by the relative solubilities, the nature of counterions, lattice energies, and related factors. The use of MeOH as reaction solvent is crucial for clean product formation; oily products were obtained when the reaction was performed in EtOH, DMF or MeCN, whereas no significant reaction was observed when the solvent was CH_2Cl_2 or $CHCl_3$.

The same methodology was employed for the synthesis of $[Mn_6O_3(N_3)_5(mpko)_6(H_2O)]{\cdot}4.25H_2O$ (**2**·$4.25H_2O$), the only difference being the introduction into the reaction of NaO_2CMe. The latter was intended to divert the reaction to a carboxylate-containing product different from **1**, but the main, isolated product was carboxylate-free **2**; further investigation of this reaction system did not produce a different product. Nevertheless, complex **2** is different from **1** in containing a higher content of azide ligands and thus yielding a neutral compound.

Description of Structures

Complex **1**·$5H_2O$ crystallizes in the triclinic space group $P\bar{1}$, with the $[Mn_6O_3(N_3)_3(mpko)_6(H_2O)_3]^{2+}$ cation in a general position. The structure of the cation and a stereopair

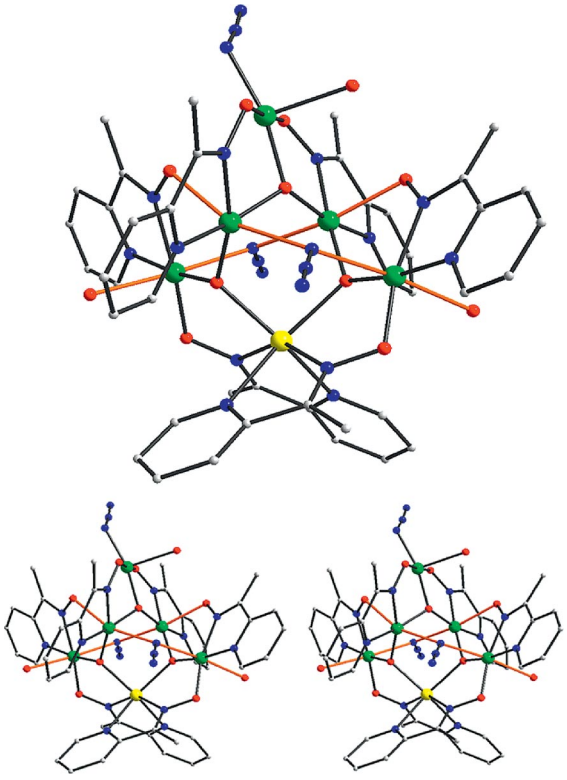

Figure 1. The structure (top) and a stereopair (bottom) of the cation of complex **1**, emphasizing the four Mn^{III} Jahn–Teller axes as brown bonds. Hydrogen atoms have been omitted for clarity. Color scheme: Mn^{II} yellow; Mn^{III} green; O red; N blue; C grey.

are shown in Figure 1, and two views of its core are presented in Figure 2. Selected interatomic distances and angles are listed in Table 1.

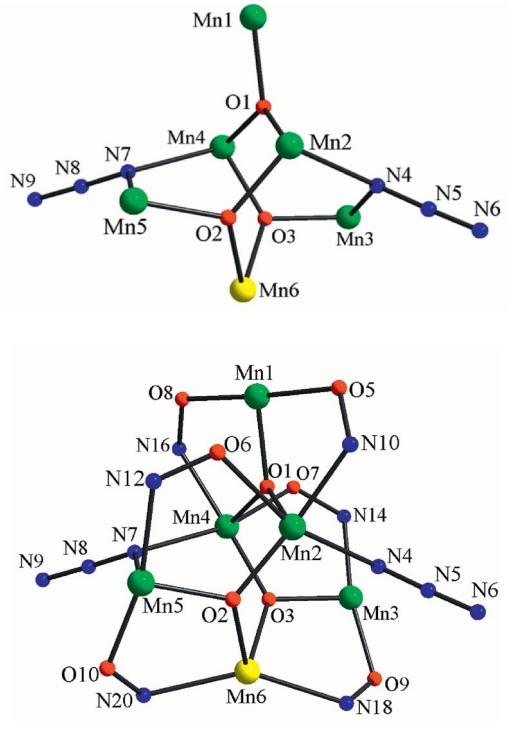

Figure 2. Labeled PovRay representation of the core of complex **1** as $[Mn_6(\mu_3\text{-}O)_3(\mu\text{-}N_3)_2]^{9+}$ (top) and more-complete $[Mn_6(\mu_3\text{-}O)_3(\mu\text{-}N_3)_2(\mu\text{-}OR')_6]^{3+}$ (bottom). Color scheme as in Figure 1.

There is a $[Mn_6O_3(N_3)_2]^{9+}$ core consisting of one Mn^{II} (Mn6) and five Mn^{III} atoms bridged by three μ_3-O^{2-} and two η^2:μ (end-on) N_3^- ions (Figure 2, top); additional ligation about the $[Mn_6O_3(N_3)_2]^{9+}$ core is provided by six tridentate, η^1:η^1:η^1:μ oximate ligands to give an overall $[Mn_6(\mu_3\text{-}O)_3(\mu\text{-}N_3)_2(\mu\text{-}OR')_6]^{3+}$ core [R′ = (py)C(Me)N; Figure 2, bottom]. The $[Mn_6O_3(N_3)_2]^{9+}$ core can be conveniently described as three oxide-centered $[Mn_3O]$ triangular units, each sharing two of its vertices with the neighboring triangular units. Each mpko$^-$ group is an *N*,*N*-chelate to a Mn atom and bridges with its O atom to an adjacent Mn^{III} atom. As a result, two edges of each triangular unit are bridged by a bidentate N–O$^-$ oximato group, with the Mn–N–O–Mn torsion angles lying in the 6.9–33.9° range. Ligation is completed by one terminal N_3^- (on Mn1) and three terminal H_2O (on Mn1, Mn3, Mn5) ligands. All Mn atoms are six-coordinate with near-octahedral geometry, except Mn1 which is five-coordinate with distorted square pyramidal geometry (τ = 0.17, where τ is 0 and 1 for ideal square-pyramidal and trigonal-bipyramidal geometries, respectively).[22]

The Mn oxidation states were obvious from the metric parameters (Table 1) and charge-balance considerations, and were confirmed by bond valence sum (BVS) calculations (Table 2)[23] and the Jahn–Teller (JT) distortions (axial elongations) at the Mn^{III} atoms (Mn2, Mn3, Mn4, Mn5); the JT elongated Mn^{III}–O bonds are at least 0.1–0.2 Å longer than the other Mn^{III}–O bonds. As expected, the JT elongation axes avoid the Mn^{III}–O^{2-} bonds, the shortest and strongest in the cation,[8] pointing toward the end-on azides.

Table 1. Selected interatomic distances [Å] and angles [°] for **1**·5H_2O.

Mn1–O1	1.891(9)	Mn5–N12	2.047(1)
Mn1–O8	1.950(1)	Mn5–N13	2.055(1)
Mn1–O5	1.955(1)	Mn5–N7	2.273(1)
Mn1–N1	1.991(1)	Mn5–O12	2.280(1)
Mn1–O4	2.203(1)	Mn6–O2	2.133(1)
Mn2–O2	1.858(9)	Mn6–O3	2.165(1)
Mn2–O1	1.887(9)	Mn6–N18	2.195(1)
Mn2–N10	2.006(1)	Mn6–N20	2.201(1)
Mn2–N11	2.029(1)	Mn6–N21	2.285(1)
Mn2–O6	2.226(1)	Mn6–N19	2.320(1)
Mn2–N4	2.328(1)	Mn1···Mn2	3.078(3)
Mn3–O3	1.861(8)	Mn1···Mn3	5.173(9)
Mn3–O9	1.898(9)	Mn1···Mn4	3.259(7)
Mn3–N14	2.016(1)	Mn1···Mn5	4.734(1)
Mn3–N15	2.044(1)	Mn1···Mn6	5.694(6)
Mn3–O11	2.306(1)	Mn2···Mn3	4.004(6)
Mn3–N4	2.354(1)	Mn2···Mn4	3.337(8)
Mn4–O3	1.830(9)	Mn2···Mn5	3.184(3)
Mn4–O1	1.865(1)	Mn2···Mn6	3.440(7)
Mn4–N16	2.019(1)	Mn3···Mn4	3.162(3)
Mn4–N17	2.033(1)	Mn3···Mn5	5.803(8)
Mn4–O7	2.237(9)	Mn3···Mn6	3.348(9)
Mn4–N7	2.357(1)	Mn4···Mn5	3.970(6)
Mn5–O2	1.862(9)	Mn4···Mn6	3.447(7)
Mn5–O10	1.904(1)	Mn5···Mn6	3.357(6)
Mn1–O1–Mn2	109.1(5)	Mn3–O3–Mn4	117.9(4)
Mn1–O1–Mn4	120.4(5)	Mn3–O3–Mn6	112.3(4)
Mn2–O1–Mn4	125.6(5)	Mn4–O3–Mn6	119.0(4)
Mn2–O2–Mn5	117.7(5)	Mn2–N4–Mn3	117.6(5)
Mn2–O2–Mn6	118.9(4)	Mn4–N7–Mn5	118.1(5)
Mn5–O2–Mn6	114.2(4)		

Finally, there are various hydrogen bonds between the Mn_6 cations and ClO_4^- anions, and some of these serve to bridge separate cations: for example, the water molecule (O11) on Mn3 forms a hydrogen bond to the ClO_4^- anion (O11···O16 2.874 Å), which in turn forms a hydrogen bond to a neighboring water molecule (O12) attached to Mn5 (O13···O12 2.732 Å).

Complex **2**·4.25H_2O crystallizes in the monoclinic space group $P2_1/n$. Selected interatomic distances and angles are listed in Table 3. The molecular structure of **2** (Figure 3) is very similar to that of **1**, with the major differences located at the terminal ligands and the absence of ClO_4^- anions in the lattice. The terminal ligation now consists of one H_2O molecule (on Mn5) and three azide ions (on Mn4, Mn5, Mn6). The oxidation states of the Mn ions in **2** are the same as in the case of **1**, with the Mn^{II} ion being Mn2, as established by charge balance considerations, the presence of JT elongations on Mn^{III} ions, and BVS. calculations[23] (provided in Table 2). As for **1**, there are again hydrogen bonds, now involving the lattice water molecules, and some again serve to link adjacent Mn6 molecules. All Mn ions are six-coordinate with distorted octahedral geometry, except Mn5 which is five-coordinate with distorted square-pyramidal geometry (τ = 0.21). The Mn–N–O–Mn torsion

Table 2. Bond valence sum (BVS)[a] calculations for the Mn and selected O atoms in **1** and **2**.

	1			**2**		
Atom	Mn^{II}	Mn^{III}	Mn^{IV}	Mn^{II}	Mn^{III}	Mn^{IV}
Mn1	2.90	*2.70*	2.77	3.31	*3.11*	3.13
Mn2	3.33	*3.13*	3.15	*2.13*	2.02	2.00
Mn3	3.18	*2.99*	3.01	3.30	*3.09*	3.12
Mn4	3.37	*3.17*	3.19	3.29	*3.11*	3.10
Mn5	3.18	*2.99*	3.01	3.09	*2.87*	2.94
Mn6	*2.08*	1.97	1.95	3.30	*3.12*	3.12
	1			**2**		
Atom	BVS	Assignment		Atom	BVS	Assignment
O1	1.91	O^{2-} [b]		O7	1.96	O^{2-} [b]
O2	1.70	O^{2-} [b]		O8	1.70	O^{2-} [b]
O3	1.73	O^{2-} [b]		O10	1.74	O^{2-} [b]
O4	0.27	H_2O [b]		O9	0.30	H_2O [b]
O11	0.21	H_2O [b]				
O12	0.22	H_2O [b]				

[a] The value printed in *italics* is the one closest to the charge for which it was calculated. The oxidation state of a particular atom can be taken as the whole number nearest to the value printed in *italics*. [b] An O BVS in the ca. 1.7–2.0, ca. 1.0–1.2 and ca. 0.2–0.4 ranges is indicative of non-, single- and double-protonation, respectively.

angles in **2** lie in the 5.7–30.7° range, slightly smaller than the corresponding values in complex **1**. The main structural differences between **1** and **2** are summarized in Table 4, where it can be seen that the most significant differences are in the Mn–N–O–Mn torsion angles and the displacement of the μ_3-O^{2-} ions out of the Mn_3 planes.

Table 3. Selected interatomic distances [Å] and angles [°] for **2**·4.25H_2O.

Mn1–O10	1.854(5)	Mn5–N22	1.946(7)
Mn1–O7	1.879(5)	Mn5–O2	1.953(5)
Mn1–N2	2.020(6)	Mn5–O4	1.966(5)
Mn1–N1	2.039(6)	Mn5–O9	2.160(6)
Mn1–O1	2.248(5)	Mn6–O10	1.856(4)
Mn1–N13	2.311(6)	Mn6–O6	1.911(5)
Mn2–O10	2.112(5)	Mn6–N12	2.015(6)
Mn2–O8	2.132(5)	Mn6–N11	2.043(6)
Mn2–N4	2.184(6)	Mn6–N25	2.237(9)
Mn2–N6	2.193(6)	Mn6–N16	2.337(6)
Mn2–N5	2.314(6)	Mn1···Mn2	3.426(2)
Mn2–N3	2.318(7)	Mn1···Mn3	3.306(4)
Mn3–O8	1.848(5)	Mn1···Mn4	4.000(2)
Mn3–O7	1.887(5)	Mn1···Mn5	3.250(2)
Mn3–N8	2.018(6)	Mn1···Mn6	3.175(2)
Mn3–N7	2.048(6)	Mn2···Mn3	3.467(2)
Mn3–O3	2.211(5)	Mn2···Mn4	3.319(2)
Mn3–N16	2.346(6)	Mn2···Mn5	5.735(2)
Mn4–O8	1.877(4)	Mn2···Mn6	3.359(2)
Mn4–O5	1.914(5)	Mn3···Mn4	3.207(3)
Mn4–N10	2.013(7)	Mn3···Mn5	3.118(2)
Mn4–N9	2.051(6)	Mn3···Mn6	4.005(2)
Mn4–N19	2.210(6)	Mn4···Mn5	4.843(2)
Mn4–N13	2.313(6)	Mn4···Mn6	5.815(4)
Mn5–O7	1.851(5)	Mn5···Mn6	5.201(2)
Mn1–O7–Mn3	122.8(3)	Mn1–O10–Mn2	119.4(2)
Mn1–O7–Mn5	121.2(2)	Mn1–O10–Mn6	117.7(2)
Mn3–O7–Mn5	113.1(2)	Mn2–O10–Mn6	115.5(2)
Mn2–O8–Mn3	121.0(2)	Mn1–N13–Mn4	119.8(2)
Mn2–O8–Mn4	111.6(2)	Mn3–N16–Mn6	117.6(2)
Mn3–O8–Mn4	118.8(3)		

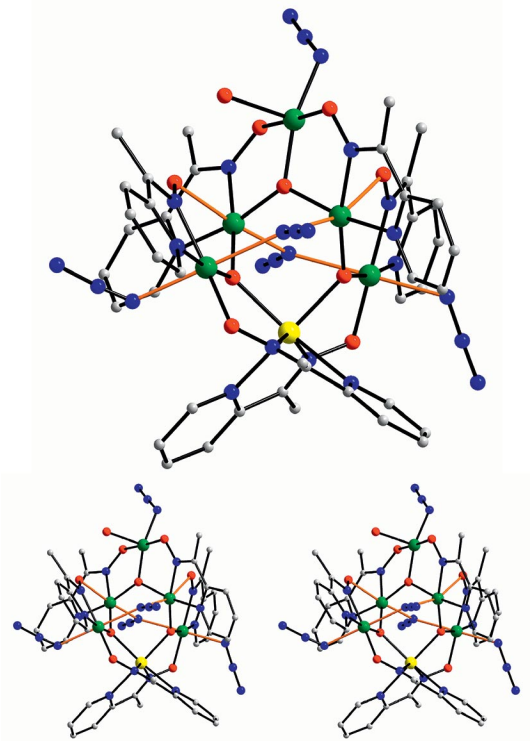

Figure 3. The molecular structure (top) and a stereopair view (bottom) of complex **2**, emphasizing the four Mn^{III} Jahn–Teller axes. Hydrogen atoms have been omitted for clarity. Color scheme as in Figure 1.

There have been a large number of Mn_6 complexes reported in the literature, most of them being mixed-valent ($Mn^{II/III}$) or Mn^{III} systems,[13a,13b,13e,13f,24] as well as few exceptional $Mn^{II/III/IV}$ and $Mn^{III/IV}$ species,[25] and these possess a wide variety of metal topologies such as edge-sharing bitetrahedra, octahedra, fused triangles, etc. Compounds **1**

Table 4. Structural differences between complexes **1** and **2**.

Parameter	**1**	**2**
Mn–(μ-N_3)–Mn [°]	117.6	117.6
	118.1	119.8
Mn–(μ_3-O^{2-}) [Å][a]	1.881	1.872
	1.952	1.952
	1.951	1.941
Mn–(μ_3-O^{2-})–Mn [°][a]	118.4	119.0
	116.4	117.2
	117.0	117.5
d [Å][b]	0.241	0.187
	0.371	0.330
	0.343	0.306
Mn–(N–O^-)–Mn [°][c]	19.3	17.4

[a] Average value per triangular subunit. [b] *d* is the distance [Å] of each μ_3-O^{2-} ion from the corresponding Mn_3 plane. [c] Average value from the six mpko$^-$ ligands.

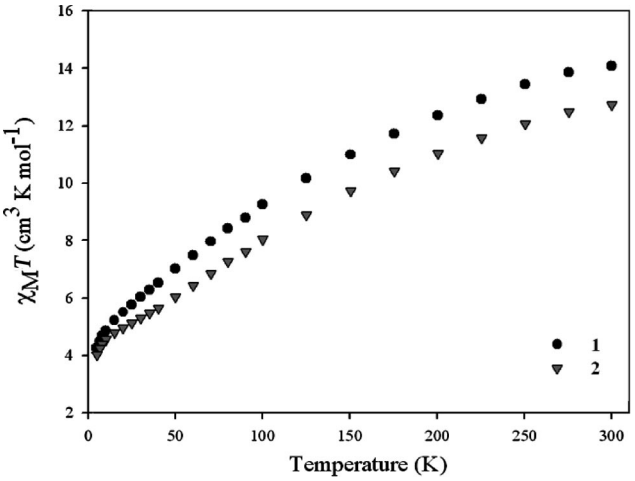

Figure 4. $\chi_M T$ vs. *T* for complexes **1** (●) and **2** (▼) in the 5.0–300 K range.

and **2** are only the second and third Mn_6 complexes at the $Mn^{II}Mn^{III}_5$ level, and the first with the $[Mn^{II}Mn^{III}_5(\mu_3\text{-}O)_3(\mu\text{-}N_3)_2]^{9+}$ core comprising three vertex-fused triangular units. The one previous Mn_6 at this oxidation level is $Na_2[Mn_6(\mu_6\text{-}O)(thme)_4(N_3)_5(H_2O)]$, which has a core consisting of a Mn_6 octahedron with a central μ_6-O^{2-} ion, and bridging alkoxide groups from the $thme^{3-}$ [thmeH_3 = 1,1,1-tris(hydroxymethyl)ethane] anions.[26]

Complexes **1** and **2** join a relatively small family of Mn compounds with mpkoH and/or mpko$^-$ ligands, currently comprising $[Mn(O_2CPh)_2(mpkoH)_2]$ (Mn^{II}),[27] $[Mn_3O(O_2CR)_3(mpko)_3]^+$ ($3Mn^{III}$),[17] $[Mn_3(OMe)_2(mpko)_4Br_2]$ ($2Mn^{II}$, Mn^{IV}),[13d] $[Mn^{II}_2Mn^{III}_6O_4(OMe)(mpko)_9(mpkoH)]^{4+}$ ($2Mn^{II}$, $6Mn^{III}$),[13d] and $[Mn_8O_2(OH)_2(O_2CPh)_{10}(mpko)_4]$ ($4Mn^{II}$, $4Mn^{III}$).[27]

Magnetochemistry

Solid-state, variable-temperature dc magnetic susceptibility (χ_M) data were collected on vacuum-dried microcrystalline samples of complexes **1** and **2**, suspended in eicosane to prevent torquing, in the 5.0–300 K temperature range in a 0.1 T (1000 G) magnetic field. The obtained data are plotted as $\chi_M T$ vs. *T* in Figure 4, and it can be seen that the plots are similar, but not identical, for the two complexes. The $\chi_M T$ values at 300 K (14.08 and 12.72 cm^3 mol^{-1} K for **1** and **2**, respectively) are both much lower than the expected room temperature $\chi_M T$ value for one Mn^{II} and five Mn^{III} ions (19.38 cm^3 mol^{-1} K with g = 2), indicating the presence of dominant antiferromagnetic interactions, and they steadily decrease with decreasing temperature.[28] The $\chi_M T$ values at 5 K (4.26 and 4.01 cm^3 mol^{-1} K for **1** and **2**, respectively) both suggest an S = 5/2 ground state with $g = 1.94 \pm 3$; the spin-only value for S = 5/2 is 4.38 cm^3 mol^{-1} K. The overall similar behavior for **1** and **2** is as expected from their essentially isostructural magnetic cores.

Given the low symmetry of the Mn_6 clusters and the resulting number of inequivalent exchange constants, it is not possible to apply the Kambe method[29] to determine the individual pairwise Mn_2 exchange interaction parameters. We therefore concentrated instead on characterizing the ground state spin, *S*, and the zero-field splitting parameter, *D*, by collecting magnetization (*M*) data in the 1–50 kG magnetic field (*H*) and 1.8–10.0 K temperature ranges. The obtained data are shown as reduced magnetization ($M/N\mu_B$) vs. H/T plots in Figure 5 for complex **1**, where *N* is Avogadro's number and μ_B is the Bohr magneton. We fit the data using the program MAGNET[30] to a model that assumes that only the ground state is populated at these temperatures and magnetic fields, includes isotropic Zeeman interactions and axial zero-field splitting ($D\hat{S}_z^2$), and incorporates a full powder average. The corresponding spin Hamiltonian is given by Equation (1), where $\hat{S}_z$ is the easy-axis spin operator and μ_0 is the vacuum permeability. The last term in Equation (1) is the Zeeman energy associated with an applied magnetic field. For **1**, the best fit (solid lines in Figure 5) gave S = 5/2, D = –1.4(3) cm^{-1}, and g = 1.99(1); the fit was noticeably worse when positive values of *D* were employed.

$$H = D\hat{S}_z^2 + g\mu_B\mu_0\hat{S}\cdot H \quad (1)$$

Alternative fits with S = 3/2 or 7/2 were rejected because they gave unreasonable values of *g*. The *D* value carries high uncertainty and is not to be taken as accurate; nevertheless, it appears larger than normally observed for Mn_x clusters, which is consistent with the almost parallel orientation of the four Mn^{III} JT axes and the *z* axis of the five-coordinate Mn^{III} atom, which will lead to a significant overall molecular anisotropy. For complex **2**, an acceptable fit was not obtained to our satisfaction, even though **1** and **2** have such similar structures, and we assume this is due to lower-lying excited states than for **1**. We have come across cases before where two structurally similar complexes differ significantly in the quality of the reduced magnetization fits.[10d,10e]

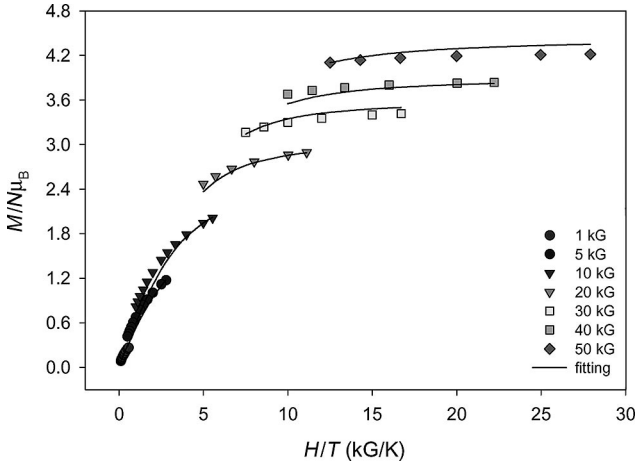

Figure 5. Reduced magnetization ($M/N\mu_B$) vs. H/T plot for complex **1**. The solid lines are the fit of the data; see the text for the fit parameters.

As we and others have described before on multiple occasions,[7–18] alternating-current (ac) susceptibility studies are a powerful complement to dc studies for determining the ground state of a system, because they preclude any complications arising from the presence of a dc field. We thus chose to carry out ac studies on complexes **1** and **2** in the 1.8–15 K range using a 3.5 G ac field oscillating at frequencies in the 50–1000 Hz range. If the magnetization vector can relax fast enough to keep up with the oscillating field, then there is no imaginary (out-of-phase) susceptibility signal (χ''_M), and the real (in-phase) susceptibility (χ'_M) is equal to the dc susceptibility. However, if the barrier to magnetization relaxation is significant compared to thermal energy (kT), then the in-phase signal decreases and a non-zero, frequency-dependent χ''_M signal appears, which is suggestive of the superparamagnetic-like properties of a SMM. For complexes **1** and **2**, the in-phase (Figures 6 and 7, top, respectively) and out-of-phase (Figures 6 and 7, bottom, respectively) ac signals are very similar, both showing a decrease in $\chi'_M T$ with lowering of the temperature, consistent with decreasing population of low-lying excited states with S greater on average than that of the ground state; a frequency-dependent split becomes evident at temperatures below ca. 4 K. The latter is followed by a concomitant appearance of χ''_M signals, which are also frequency-dependent and whose maxima lie below the operating minimum temperature of our SQUID instrument (1.8 K). This behavior is indicative of slow magnetization relaxation, suggesting **1** and **2** to possibly be new SMMs, but ones with rather small relaxation barriers. Further confirmation of the SMM behavior would require single-crystal studies on a micro-

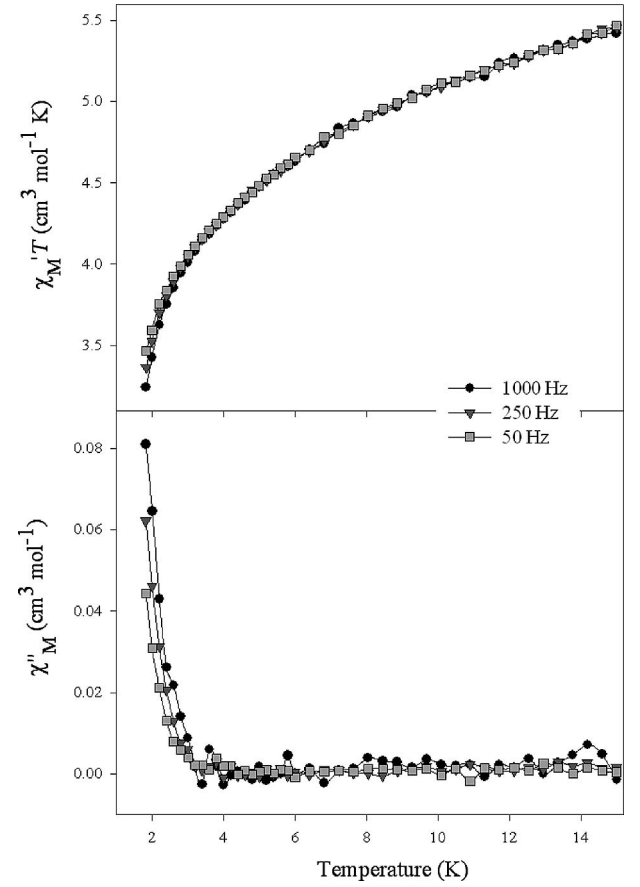

Figure 6. Plots of the in-phase (χ_M') as $\chi_M'T$ (top), and out-of-phase (χ_M'') (bottom) ac magnetic susceptibilities vs. T in a 3.5 G field oscillating at the indicated frequencies for complex **1**.

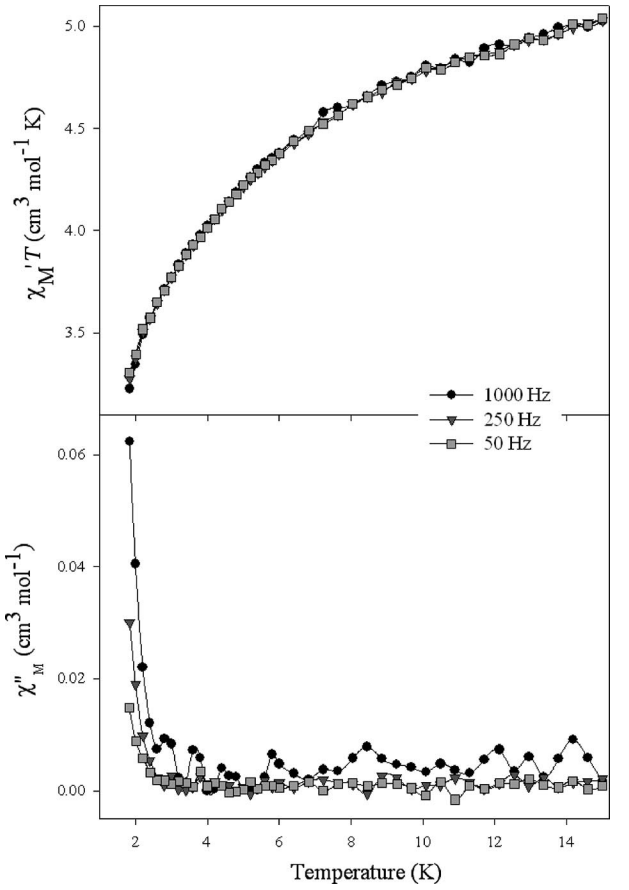

Figure 7. Plots of the in-phase (χ_M') as $\chi_M'T$ (top), and out-of-phase (χ_M'') (bottom) ac magnetic susceptibilities vs. T in a 3.5 G field oscillating at the indicated frequencies for complex **2**.

SQUID down to 40 mK,[31] but this was not pursued because there are now many SMMs with such small relaxation barriers.

The in-phase $\chi'_M T$ data support the conclusion from the dc magnetization data that **1** and **2** have an $S = 5/2$ ground state. The $\chi'_M T$ shows a near-linear decrease above ca. 7 K, which extrapolates to the 4.0–4.5 $cm^3 mol^{-1} K$ region at 0 K consistent with an $S = 5/2$ ground state, before showing a steeper decrease assignable to a combination of the anisotropy, Zeeman effects, and very weak intermolecular interactions mediated by the hydrogen-bonds in the structure. Note that the spin-only ($g = 2.0$) $\chi'_M T$ values for $S = 3/2$, 5/2 and 7/2 ground states are 1.88, 4.38, and 7.88 $cm^3 mol^{-1} K$, respectively.[28]

The $S = 5/2$ ground states of **1** and **2** have not been previously seen in Mn_6 clusters. Because **1** and **2** contain fused triangular units, textbook examples of a topology that can give spin frustration effects (competing exchange interactions), we conclude that the $S = 5/2$ ground state is arising from spin frustration within the triangular sub-units.[9a,28] There are thus various possible coupling schemes and resulting intermediate spin alignments at some Mn atoms that could yield an $S = 5/2$ ground state, making it difficult to rationalize the observed value in a unique manner without recourse to theoretical calculations. Some coupling schemes can be ruled out, however, such as the ferromagnetic $J(Mn^{III}Mn^{III})$ and antiferromagnetic $J(Mn^{II}Mn^{III})$ possibility, which would give an $S = 15/2$ ground state.

Conclusions

The combined use of 2-pyridyl oximes and azide ligands in Mn non-carboxylate chemistry has afforded two new, mixed-valence(II/III) Mn_6 clusters with an unprecedented metal topology. The complexes $[Mn_6O_3(N_3)_3(mpko)_6(H_2O)_3](ClO_4)_2$ (**1**) and $[Mn_6O_3(N_3)_5(mpko)_6(H_2O)]$ (**2**) contain the anion of methyl 2-pyridyl ketone oxime ($mpko^-$), together with both terminal (η^1) and end-on bridging (η^2:μ) azide groups. Even though **1** and **2** have a small ground state spin of $S = 5/2$, they also possess a significant and negative zero-field splitting parameter, D, which can be rationalized as due to the near-parallel alignment of the four Mn^{III} JT axes, and the z axis of the five-coordinate square pyramidal Mn. This combination of S and D is sufficient to give frequency-dependent, out-of-phase ac signals suggestive of SMMs, but ones with a low barrier; the very similar magnitudes and temperature profiles of the out-of-phase ac signals for **1** and **2** are as expected for the near-isostructural compounds and supports the behavior as arising from the Mn_6 complexes rather than adventitious impurities. Further, as mentioned, we anticipate only very weak intermolecular interactions mediated by the hydrogen-bonding in the crystal structures, so rule out the possibility that the out-of-phase signals are coming from single-chain magnet (SCM) behavior; in any case; the intermolecular interactions will undoubtedly be antiferromagnetic rather than the ferromagnetic required for an SCM (from identical repeating units, at least). Finally, we anticipate a variety of new metal clusters of different nuclearities and structural topologies to be attained as we extend the use in cluster chemistry of mpkoH and N_3^- combinations, as well as others. Further work is in progress.

Experimental Section

Materials and Physical Measurements: All manipulations were performed under aerobic conditions using chemicals and solvents as received, unless otherwise stated. mpkoH was prepared as described elsewhere.[32]

Warning: *Azide and perchlorate salts are potentially explosive; such compounds should be synthesized and used in small quantities, and treated with utmost care at all times.*

Infrared spectra were recorded on KBr pellets with a Nicolet Nexus 670 FTIR spectrometer in the 400–4000 cm^{-1} range. Elemental analyses (C,H,N) were performed by the in-house facilities of the University of Florida Chemistry Department. Variable-temperature dc and ac magnetic susceptibility data were collected with a Quantum Design MPMS-XL SQUID magnetometer equipped with a 7 T magnet and operating in the 1.8–300 K range. Samples were embedded in eicosane to prevent torquing. Magnetization vs. field and temperature data were fit using the program MAGNET.[30] Pascal's constants were used to estimate the diamagnetic corrections, which were subtracted from the experimental susceptibilities to give the molar paramagnetic susceptibilities (χ_M).

$[Mn_6O_3(N_3)_3(mpko)_6(H_2O)_3](ClO_4)_2$ (1): Solid NaN_3 (0.07 g, 1.0 mmol) was added to a stirred solution of mpkoH (0.14 g, 1.0 mmol) and NEt_3 (0.14 mL, 1.0 mmol) in MeOH (30 mL). After 10 min of stirring, solid $Mn(ClO_4)_2 \cdot 6H_2O$ (0.36 g, 1.0 mmol) was slowly added, and the resulting solution soon became dark brown. The reaction mixture was kept under magnetic stirring for another 30 min. The solution was then filtered and Et_2O was slowly diffused into it over a period of 2 d, during which time large brown crystals of $\mathbf{1} \cdot 5H_2O$ grew. The crystals were maintained in the mother liquor for X-ray crystallography and other single-crystal studies, or collected by filtration, washed with cold MeOH (2×3 mL) and Et_2O (2×5 mL), and dried under vacuum over silica gel; the yield was ca. 50% (0.13 g). The dried solid analyzed as solvent-free. $C_{42}H_{48}Cl_2Mn_6N_{21}O_{20}$ (1567.63): calcd. C 32.10, H 3.06, N 18.94; found C 32.18, H 3.09, N 18.76. IR (KBr): $\tilde{\nu}$ = 3440 (mb), 2925 (w), 2363 (w), 2048 (vs), 1636 (m), 1601 (m), 1470 (w), 1381 (w), 1333 (mb), 1263 (w), 1152 (vs), 1082 (vsb), 782 (m), 705 (m), 623 (s), 587 (m), 560 (m), 494 (w), 462 (w) cm^{-1}.

$[Mn_6O_3(N_3)_5(mpko)_6(H_2O)]$ (2): Solid NaN_3 (0.07 g, 1.0 mmol) was added to a stirred solution of mpkoH (0.27 g, 2.0 mmol), NEt_3 (0.33 mL, 2.3 mmol), and NaO_2CMe (0.08 g, 1.0 mmol) in MeOH (30 mL). After 10 min of stirring, solid $Mn(ClO_4)_2 \cdot 6H_2O$ (0.72 g, 2.0 mmol) was added, and the resulting solution soon became dark brown. The reaction mixture was kept under magnetic stirring for another 30 min. The solution was then filtered and Et_2O was slowly diffused into it over a period of 2 d, during which time large brown crystals of $\mathbf{2} \cdot 4.25H_2O$ grew. The crystals were maintained in the mother liquor for X-ray crystallography and other single-crystal studies, or collected by filtration, washed with cold MeOH (2×3 mL) and Et_2O (2×5 mL), and dried under vacuum over silica gel; the yield was ca. 40% (0.19 g). The dried solid analyzed as solvent-free. $C_{42}H_{44}Mn_6N_{27}O_{10}$ (1416.69): calcd. C 35.72, H 3.16, N 26.58; found C 35.61, H 3.13, N 26.70. IR (KBr): $\tilde{\nu}$ = 3421 (mb), 2362 (w), 2336 (w), 2038 (vs), 1636 (m), 1600 (m), 1554 (m), 1474

(m), 1435 (mb), 1374 (w), 1333 (w), 1284 (w), 1160 (m), 1103 (m), 1068 (m), 1045 (m), 781 (m), 706 (m), 590 (mb), 564 (m), 491 (w), 455 (w) cm^{-1}.

$[Mn_6O_3(N_3)_3(mpko)_6(H_2O)_3](NO_3)_2$ (3): To a stirred solution of mpkoH (0.14 g, 1.0 mmol) and NEt_3 (0.14 mL, 1.0 mmol) in MeOH (30 mL) was added solid NaN_3 (0.07 g, 1.0 mmol). After 10 min of stirring, solid $Mn(NO_3)_2{\cdot}H_2O$ (0.20 g, 1.0 mmol) was slowly added, and the resulting solution soon became dark brown. The reaction mixture was kept under magnetic stirring for another 30 min. The solution was then filtered and Et_2O was allowed to slowly diffuse into it over a period of 4 d, during which time brown crystals of **3** grew. Due to the small size and bad quality, the crystals of **3** were not suitable for single-crystal X-ray crystallography. Thus, the crystals were collected by filtration, washed with cold MeOH (2 × 3 mL) and Et_2O (2 × 5 mL), dried under vacuum over silica gel, and characterized with elemental analysis; the yield was ca. 15% (0.04 g). The dried solid analyzed as solvent-free. $C_{42}H_{48}Mn_6N_{23}O_{18}$ (1492.62): calcd. C 33.80, H 3.24, N 21.58; found C 33.88, H 3.29, N 21.49. IR (KBr): $\tilde{\nu}$ = 3445 (mb), 2929 (w), 2050 (vs), 1632 (m), 1600 (m), 1473 (w), 1385 (vs), 1323 (m), 1266 (w), 1153 (s), 1050 (s), 855 (m), 700 (m), 635 (m), 594 (m), 563 (m), 497 (w), 467 (w) cm^{-1}.

X-ray Crystallography and Solution of Structures: Suitable crystals of **1**·5H_2O and **2**·4.25H_2O were attached to glass fibers using silicone grease and transferred to a goniostat where they were cooled to 173 and 100 K, respectively, for data collection. An initial search of reciprocal space revealed a triclinic cell for **1**·5H_2O, and a monoclinic cell for **2**·4.25H_2O; the choice of space groups $P\bar{1}$ and $P2_1/n$, respectively, was confirmed by the subsequent solution and refinement of the structures.

Data for complex **1**·5H_2O were collected with a Siemens SMART PLATFORM equipped with a CCD area detector and a graphite monochromator utilizing Mo-K_α radiation (λ = 0.71073 Å). The crystal was a poor diffractor; many crystals from multiple presentations were studied, but a better quality crystal could not be found. Cell parameters were refined using up to 8192 reflections. A full sphere of data (1850 frames) was collected using the ω-scan method (0.3° frame width). The first 50 frames were remeasured at the end of data collection to monitor instrument and crystal stability (maximum correction on I was <1%). Absorption corrections by integration were applied based on measured indexed crystal faces. The structure was solved by direct methods in SHELXTL6,[33] and refined on F^2 using full-matrix least-squares. The non-H atoms were treated anisotropically, except for those of the disordered anions and lattice water molecules, whereas the H atoms were placed in calculated, ideal positions and refined as riding on their respective C atoms.

Data for **2**·4.25H_2O were collected with an Oxford Diffraction Xcalibur-3 diffractometer equipped with a Sapphire CCD area detector. Cell parameters were refined using 9168 reflections (3.2° ≤ θ ≤ 30.2°). Data (792 frames) were collected using the ω-scan method (0.60° frame). Empirical absorption corrections (multi-scan based on symmetry-related measurements) were applied using CrysAlis RED software.[34] The structure was solved by direct methods using SIR 2002[35] and refined on F^2 using full-matrix least-squares with SHELXL-97.[36] All non-H atoms were refined anisotropically. All H atoms attached to C atoms were placed in calculated, ideal positions and refined as riding on their respective C atoms. The programs used were CrysAlis CCD[34] for data collection, CrysAlis RED[34] for cell refinement and data reduction, WINGX[37] and PLATON[38] for crystallographic calculations, and MERCURY[39] and DIAMOND[40] for molecular graphics.

The asymmetric unit of **1**·5H_2O consists of a Mn_6 dicationic cluster, two disordered ClO_4^- anions, and five H_2O molecules of crystallization. The ClO_4^- anions were refined in two parts with their site-occupation factors dependently refined (65:35% for Cl1, and 57:43% for Cl2); their structures were additionally constrained to maintain ideal geometries. None of the water protons could be located in difference Fourier maps and thus were not included in the final refinements. A total of 811 parameters were refined in the final cycle of refinement using 4501 reflections with $I > 2\sigma(I)$.

For complex **2**·4.25H_2O, the asymmetric unit contains a complete Mn_6 cluster and four and one quarter H_2O molecules of crystallization. The terminally-bound azide groups exhibited large thermal ellipsoids due to positional disorder that could not be resolved into distinct sites. A total of 844 parameters were refined in the final cycle of refinement using 6157 reflections with $I > 2\sigma(I)$.

Unit cell parameters and structure solution and refinement data for both complexes are listed in Table 5.

Table 5. Crystallographic data for complexes **1**·5H_2O and **2**·4.25H_2O.

	1·5H_2O	**2**·4.25H_2O
Formula[a]	$C_{42}H_{58}Cl_2Mn_6N_{21}O_{25}$	$C_{42}H_{52.5}Mn_6N_{27}O_{14.25}$
M [g mol^{-1}][a]	1657.63	1493.19
Crystal system	triclinic	monoclinic
Space group	$P\bar{1}$	$P2_1/n$
a [Å]	13.173(3)	15.3962(4)
b [Å]	15.530(3)	25.5091(8)
c [Å]	16.658(4)	16.2520(4)
α [°]	85.820(4)	90
β [°]	75.620(3)	95.838(2)
γ [°]	80.578(4)	90
V [Å^3]	3254.7(12)	6349.8(3)
Z	2	4
T [K]	173(2)	100(2)
λ [Å][b]	0.71073	0.71069
$\rho_{calcd.}$ [g cm^{-3}]	1.691	1.551
μ [mm^{-1}]	1.304	1.236
Measd./independent (R_{int}) reflections	14722/8505 (0.1825)	40357/11121 (0.0845)
Obsd. reflections [$I > 2\sigma(I)$]	4501	6157
R_1[c,d]	0.0955	0.0710
wR_2[e]	0.2298	0.1815
GOF on F^2	1.101	0.963
$(\Delta\rho)_{max., min.}$ [e Å^{-3}]	1.541, –1.225	1.264, –0.634

[a] Including solvate molecules. [b] Graphite monochromator. [c] $I > 2\sigma(I)$. [d] $R_1 = \Sigma(||F_o| - |F_c||)/\Sigma|F_o|$. [e] $wR_2 = \{\Sigma[w(F_o^2 - F_c^2)^2]/\Sigma[w(F_o^2)^2]\}^{1/2}$, $w = 1/[\sigma^2(F_o^2) + (ap)^2 + bp]$, where $p = [\max.(F_o^2, 0) + 2F_c^2]/3$.

CCDC-739936 (for **1**·5H_2O) and CCDC-739935 (for **2**·4.25H_2O) contain the supplementary crystallographic data for this paper. These data can be obtained free of charge from The Cambridge Crystallographic Data Centre via www.ccdc.cam.ac.uk/data_request/cif.

Supporting Information (see also the footnote on the first page of this article): Plot magnetization (M) vs. field (H) and temperature (T) data.

Acknowledgments

This work was supported by the Cyprus Research Promotion Foundation and the USA National Science Foundation (CHE-0910472).

[1] a) S. J. Lippard, *Nat. Chem. Biol.* **2006**, *2*, 504; b) S. J. Lippard, *Science* **1993**, *261*, 699; c) J. Du Bois, T. J. Mizoguchi, S. J. Lippard, *Coord. Chem. Rev.* **2000**, *200*, 443.

[2] a) K. N. Ferreira, T. M. Iverson, K. Maghlaoui, J. Barber, S. Iwata, *Science* **2004**, *303*, 1831; b) J. Barber, *Inorg. Chem.* **2008**, *47*, 1700; c) J. Yano, J. Kern, K. Sauer, M. J. Latimer, Y. Pushkar, J. Biesiadka, B. Loll, W. Saenger, J. Messinger, A. Zouni, V. K. Yachandra, *Science* **2006**, *314*, 821; d) T. G. Carrell, A. M. Tyryshkin, G. C. Dismukes, *J. Biol. Inorg. Chem.* **2002**, *7*, 2; e) R. M. Cinco, A. Rompel, H. Visser, G. Aromi, G. Christou, K. Sauer, M. P. Klein, V. K. Yachandra, *Inorg. Chem.* **1999**, *38*, 5988; f) V. K. Yachandra, K. Sauer, M. P. Klein, *Chem. Rev.* **1996**, *96*, 2927.

[3] a) X. Liu, K. Hintze, B. Lonnerdal, E. C. Theil, *Biol. Res.* **2006**, *39*, 167; b) K. Taft, G. C. Papaefthymiou, S. J. Lippard, *Science* **1993**, *259*, 1302; c) S. Macedo, C. V. Romao, E. Mitchell, P. M. Matias, M. Y. Liu, A. V. Xavier, J. LeGall, M. Teixeira, P. Lindley, M. A. Carrondo, *Nat. Struct. Biol.* **2003**, *10*, 285.

[4] a) D. Coucouvanis, *Acc. Chem. Res.* **1991**, *24*, 1; b) R. H. Holm, *Chem. Soc. Rev.* **1991**, *10*, 455; c) P. C. Dos Santos, R. Y. Igarashi, H.-I. Lee, B. M. Hoffman, L. C. Seefeldt, D. R. Dean, *Acc. Chem. Res.* **2005**, *38*, 208.

[5] For reviews, see: a) G. Christou, D. Gatteschi, D. N. Hendrickson, R. Sessoli, *MRS Bull.* **2000**, *25*, 66; b) G. Aromi, E. K. Brechin, *Struct. Bonding (Berlin)* **2006**, *122*, 1; c) G. Christou, *Polyhedron* **2005**, *24*, 2065; d) M. Murrie, D. J. Price, *Annu. Rep. Prog. Chem. Sect. A* **2007**, *103*, 20.

[6] a) R. Bircher, G. Chaboussant, C. Dobe, H. U. Güdel, S. T. Ochsenbein, A. Sieber, O. Waldmann, *Adv. Funct. Mater.* **2006**, *16*, 209; b) D. Gatteschi, R. Sessoli, *Angew. Chem. Int. Ed.* **2003**, *42*, 268; c) S. M. J. Aubin, N. R. Gilley, L. Pardi, J. Krzystek, M. W. Wemple, L.-C. Brunel, M. B. Maple, G. Christou, D. N. Hendrickson, *J. Am. Chem. Soc.* **1998**, *120*, 4991; d) H. Oshio, M. Nakano, *Chem. Eur. J.* **2005**, *11*, 5178; e) J. R. Long, in C*hemistry of Nanostructured Materials* (Ed.: P. Yang), World Scientific Publishing, Hong Kong, **2003**, pp. 291.

[7] a) M. Soler, W. Wernsdorfer, K. Folting, M. Pink, G. Christou, *J. Am. Chem. Soc.* **2004**, *126*, 2156; b) M. Soler, E. Rumberger, K. Folting, D. N. Hendrickson, G. Christou, *Polyhedron* **2001**, *20*, 1365; c) M. Murugesu, W. Wernsdorfer, K. A. Abboud, G. Christou, *Polyhedron* **2005**, *24*, 2894.

[8] For example, see: a) N. E. Chakov, S.-C. Lee, A. G. Harter, P. L. Kuhns, A. P. Reyes, S. O. Hill, N. S. Dalal, W. Wernsdorfer, K. A. Abboud, G. Christou, *J. Am. Chem. Soc.* **2006**, *128*, 6975; b) A. G. Harter, C. Lampropoulos, M. Murugesu, P. Kuhns, A. Reyes, G. Christou, N. S. Dalal, *Polyhedron* **2007**, *26*, 2320; c) C. Lampropoulos, G. Redler, S. Data, K. A. Abboud, S. Hill, G. Christou, *Inorg. Chem.* **2010**, *49*, 1325; d) R. Bagai, G. Christou, *Chem. Soc. Rev.* **2009**, *38*, 1011.

[9] a) Th. C. Stamatatos, G. Christou, *Philos. Trans. R. Soc. London, Ser. A* **2008**, *366*, 13; b) J. T. Brockman, Th. C. Stamatatos, W. Wernsdorfer, K. A. Abboud, G. Christou, *Inorg. Chem.* **2007**, *46*, 9160; c) C. J. Milios, I. A. Gass, A. Vinslava, L. Budd, S. Parsons, W. Wernsdorfer, S. P. Perlepes, G. Christou, E. K. Brechin, *Inorg. Chem.* **2007**, *46*, 6215; d) Y. Li, W. Wernsdorfer, R. Clérac, I. J. Hewitt, C. E. Anson, A. K. Powell, *Inorg. Chem.* **2006**, *45*, 2376; e) Y.-S. Ma, Y. Song, Y.-Z. Li, L.-M. Zheng, *Inorg. Chem.* **2007**, *46*, 5459.

[10] For example, see: a) C. Canada-Vilalta, M. Pink, G. Christou, *Dalton Trans.* **2003**, 1121; b) E. K. Brechin, G. Christou, M. Soler, M. Helliwell, S. J. Teat, *Dalton Trans.* **2003**, 513; c) R. Bagai, K. A. Abboud, G. Christou, *Inorg. Chem.* **2008**, *47*, 621; d) C. Lampropoulos, C. Koo, S. O. Hill, K. Abboud, G. Christou, *Inorg. Chem.* **2008**, *47*, 11180; e) C. Lampropoulos, M. Murugesu, K. A. Abboud, G. Christou, *Polyhedron* **2007**, *26*, 2129; f) A. Masello, M. Murugesu, K. A. Abboud, G. Christou, *Polyhedron* **2007**, *26*, 2276.

[11] a) Th. C. Stamatatos, G. Christou, *Inorg. Chem.* **2009**, *48*, 3308, and references cited therein; b) Th. C. Stamatatos, K. M. Poole, K. A. Abboud, W. Wernsdorfer, T. A. O'Brien, G. Christou, *Inorg. Chem.* **2008**, *47*, 5006; c) G. S. Papaefstathiou, S. P. Perlepes, A. Escuer, R. Vicente, M. Font-Bardia, X. Solans, *Angew. Chem. Int. Ed.* **2001**, *40*, 884; d) G. S. Papaefstathiou, A. Escuer, R. Vicente, M. Font-Bardia, X. Solans, S. P. Perlepes, *Chem. Commun.* **2001**, 2414; e) A. K. Boudalis, B. Donnadieu, V. Nastopoulos, J. M. Clemente-Juan, A. Mari, Y. Sanakis, J.-P. Tuchagues, S. P. Perlepes, *Angew. Chem. Int. Ed.* **2004**, *43*, 2266; f) Th. C. Stamatatos, A. Vinslava, K. A. Abboud, G. Christou, *Chem. Commun.* **2009**, 2839; g) E. E. Moushi, Th. C. Stamatatos, W. Wernsdorfer, V. Nastopoulos, G. Christou, A. J. Tasiopoulos, *Inorg. Chem.* **2009**, *48*, 5049.

[12] For reviews, see: a) A. J. Tasiopoulos, S. P. Perlepes, *Dalton Trans.* **2008**, 5537; b) E. K. Brechin, *Chem. Commun.* **2005**, 5141; c) Th. C. Stamatatos, C. G. Efthymiou, C. C. Stoumpos, S. P. Perlepes, *Eur. J. Inorg. Chem.* **2009**, *23*, 3361.

[13] a) C. J. Milios, S. Piligkos, E. K. Brechin, *Dalton Trans.* **2008**, 1809; b) C. J. Milios, A. Vinslava, W. Wernsdorfer, S. Maggach, S. Parsons, S. P. Perlepes, G. Christou, E. K. Brechin, *J. Am. Chem. Soc.* **2007**, *129*, 2754; c) C.-I. Yang, W. Wernsdorfer, G.-H. Lee, H.-L. Tsai, *J. Am. Chem. Soc.* **2007**, *129*, 456; d) C. C. Stoumpos, Th. C. Stamatatos, H. Sartzi, O. Roubeau, A. J. Tasiopoulos, V. Nastopoulos, S. J. Teat, G. Christou, S. P. Perlepes, *Dalton Trans.* **2009**, 1004; e) Th. C. Stamatatos, B. S. Luisi, B. Moulton, G. Christou, *Inorg. Chem.* **2008**, *47*, 1134; f) S. Khanra, T. Weyermüller, P. Chaudhuri, *Dalton Trans.* **2008**, 4885; g) C. Lampropoulos, Th. C. Stamatatos, K. A. Abboud, G. Christou, *Inorg. Chem.* **2009**, *48*, 429.

[14] A. M. Ako, I. J. Hewitt, V. Mereacre, R. Clérac, W. Wernsdorfer, C. E. Anson, A. K. Powell, *Angew. Chem. Int. Ed.* **2006**, *45*, 4926.

[15] E. E. Moushi, C. Lampropoulos, W. Wernsdorfer, V. Nastopoulos, G. Christou, A. J. Tasiopoulos, *Inorg. Chem.* **2007**, *46*, 3795.

[16] a) Th. C. Stamatatos, K. A. Abboud, S. P. Perlepes, G. Christou, *Dalton Trans.* **2007**, 3861; b) Th. C. Stamatatos, A. Escuer, K. A. Abboud, C. P. Raptopoulou, S. P. Perlepes, G. Christou, *Inorg. Chem.* **2008**, *47*, 11825.

[17] a) Th. C. Stamatatos, D. Foguet-Albiol, C. C. Stoumpos, C. P. Raptopoulou, A. Terzis, W. Wernsdorfer, S. P. Perlepes, G. Christou, *J. Am. Chem. Soc.* **2005**, *127*, 15380; b) Th. C. Stamatatos, D. Foguet-Albiol, C. C. Stoumpos, C. P. Raptopoulou, A. Terzis, W. Wernsdorfer, G. Christou, S. P. Perlepes, *Polyhedron* **2007**, *26*, 2095; c) S.-C. Lee, Th. C. Stamatatos, S. Hill, S. P. Perlepes, G. Christou, *Polyhedron* **2007**, *26*, 2225.

[18] a) C. J. Milios, C. P. Raptopoulou, A. Terzis, F. Lloret, R. Vicente, S. P. Perlepes, A. Escuer, *Angew. Chem. Int. Ed.* **2004**, *43*, 210; b) C. J. Milios, A. Vinslava, A. Whittaker, S. Parsons, W. Wernsdorfer, S. P. Perlepes, G. Christou, E. K. Brechin, *Inorg. Chem.* **2006**, *45*, 5272.

[19] a) M. A. Bolcar, S. M. J. Aubin, K. Folting, D. N. Hendrickson, G. Christou, *Chem. Commun.* **1997**, 1485; b) C. Boskovic, E. K. Brechin, W. E. Streib, K. Folting, D. N. Hendrickson, G. Christou, *Chem. Commun.* **2001**, 467; c) Th. C. Stamatatos, K. A. Abboud, W. Wernsdorfer, G. Christou, *Polyhedron* **2007**, *26*, 2042.

[20] For reviews, see: a) V. Yu. Kukushkin, A. J. L. Pombeiro, *Coord. Chem. Rev.* **1999**, *181*, 147; b) A. G. Smith, P. A. Tasker, D. J. White, *Coord. Chem. Rev.* **2003**, *241*, 61; c) P. Chaudhuri, *Coord. Chem. Rev.* **2003**, *243*, 143; d) C. J. Milios, Th. C. Stamatatos, S. P. Perlepes, *Polyhedron* **2006**, *25*, 134.

[21] a) A. Escuer, G. Aromi, *Eur. J. Inorg. Chem.* **2006**, *23*, 4721; b) E. Ruiz, J. Cano, S. Alvarez, P. Alemany, *J. Am. Chem. Soc.* **1998**, *120*, 11122.

[22] A. W. Addison, T. N. Rao, J. Reedijk, J. Rijn, G. C. Verschoor, *J. Chem. Soc., Dalton Trans.* **1984**, 1349.

[23] a) I. D. Brown, D. Altermatt, *Acta Crystallogr., Sect. B* **1985**, *41*, 244; b) W. Liu, H. H. Thorp, *Inorg. Chem.* **1993**, *32*, 4102.

[24] For example, see: a) D. M. Low, E. K. Brechin, M. Helliwell, T. Mallah, E. Riviere, E. J. L. McInnes, *Chem. Commun.* **2003**, 2330; b) M. A. Halcrow, W. E. Streib, K. Folting, G. Christou, *Acta Crystallogr., Sect. C* **1995**, *51*, 1263; c) M. Murrie, S. Parsons, R. E. P. Winpenny, *J. Chem. Soc., Dalton Trans.* **1998**, 1423; d) A. R. E. Baikie, A. J. Howes, M. B. Hursthouse, A. B. Quick, P. J. Thornton, *J. Chem. Soc., Chem. Commun.* **1986**, 1587; e) K. S. Gavrilenko, S. V. Punin, O. Cador, S. Golhen, L. Quahab, V. V. Pavlishchuk, *Inorg. Chem.* **2005**, *44*, 5903; f) M. A. Kiskin, G. G. Aleksandrov, V. N. Ikorskii, V. N. Novotortsev, I. L. Eremenko, *Inorg. Chem. Commun.* **2007**, *10*, 997; g) C.-I. Yang, Y.-J. Tsai, G. Chung, T.-S. Kuo, M. Shieh, H.-L. Tsai, *Polyhedron* **2007**, *26*, 1805.
[25] a) Th. C. Stamatatos, K. V. Pringouri, K. A. Abboud, G. Christou, *Polyhedron* **2009**, *28*, 1624; b) L. F. Jones, R. Inglis, M. E. Cochrane, K. Mason, A. Collins, S. Parsons, S. P. Perlepes, E. K. Brechin, *Dalton Trans.* **2008**, 6205.
[26] K. C. Mondal, M. G. B. Drew, P. S. Mukherjee, *Inorg. Chem.* **2007**, *46*, 5625.
[27] C. C. Stoumpos, Th. C. Stamatatos, V. Psycharis, C. P. Raptopoulou, G. Christou, S. P. Perlepes, *Polyhedron* **2008**, *27*, 3703.
[28] O. Kahn, *Molecular Magnetism*, VCH Publishers, New York, **1993**.
[29] K. J. Kambe, *J. Phys. Soc. Jpn.* **1950**, *5*, 48.
[30] E. R. Davidson, *MAGNET*, Indiana University, Bloomington, IN, USA, **1999**.
[31] W. Wernsdorfer, *Adv. Chem. Phys.* **2001**, *118*, 99.
[32] M. Orama, H. Saarinen, J. Korvenranta, *J. Coord. Chem.* **1990**, *22*, 183.
[33] *SHELXTL6*, Bruker-AXS, Madison, WI, **2000**.
[34] *CrysAlis CCD and CrysAlis RED*, Version 1.171.32.15, Oxford Diffraction Ltd., Abingdon, Oxford, England, **2008**.
[35] SIR 2002: M. C. Burla, M. Camalli, B. Carrozzini, G. L. Cascarano, C. Giacovazzo, G. Polidori, R. Spagna, *J. Appl. Crystallogr.* **2003**, *36*, 1103.
[36] G. M. Sheldrick, *SHELXL-97*, *Program for the Refinement of Crystal Structures from Diffraction Data*, University of Göttingen, Germany, **1997**.
[37] WINGX: L. J. Farrugia, *J. Appl. Crystallogr.* **1999**, *32*, 837.
[38] A. L. Spek, *PLATON-A Multipurpose Crystallographic Tool*, University of Utrecht, the Netherlands, **2008**.
[39] MERCURY: C. F. Macrae, P. R. Edgington, P. McCabe, E. Pidcock, G. P. Shields, R. Taylor, M. Towler, J. van de Streek, *J. Appl. Crystallogr.* **2006**, *39*, 453.
[40] K. Brandenburg, *DIAMOND*, Release 3.1f, Crystal Impact GbR, Bonn, Germany, **2008**.

Received: October 16, 2009
Published Online: April 9, 2010

